

Numerical study of heat transfer and chemical kinetics of solar thermochemical reactor for hydrogen production

Cite as: AIP Conference Proceedings **1984**, 020002 (2018); <https://doi.org/10.1063/1.5046586>
Published Online: 25 July 2018

Achmad Rofi Irsyad, Byunggi Kim, Doan Hong Duc, Saiful Hasmady bin Abu Hassan, and Kazuyoshi Fushinobu



View Online



Export Citation

ARTICLES YOU MAY BE INTERESTED IN

[Numerical simulation of cross flow around four circular cylinders in an in-line square configuration with the critical spacing ratio "L/D" near a plane wall](#)

AIP Conference Proceedings **1984**, 020001 (2018); <https://doi.org/10.1063/1.5046585>

[Characteristics of heat transfer on solar collector channel by using a sharp turn](#)

AIP Conference Proceedings **1984**, 020003 (2018); <https://doi.org/10.1063/1.5046587>

[Study on utilization of Indonesian non-recycled municipal solid waste as renewable solid fuel](#)

AIP Conference Proceedings **1984**, 020004 (2018); <https://doi.org/10.1063/1.5046588>

Lock-in Amplifiers
up to 600 MHz



Numerical Study of Heat Transfer and Chemical Kinetics of Solar Thermochemical Reactor for Hydrogen Production

Achmad Rofi Irsyad^{1, a)}, Byunggi Kim¹, Doan Hong Duc², Saiful Hasmady bin Abu Hassan³, Kazuyoshi Fushinobu¹

¹*Department of Mechanical and Control Engineering, Tokyo Institute of Technology, Japan*

²*University of Engineering and Technology, VNU Hanoi, Vietnam*

³*Department of Mechanical Engineering, Universiti Tenaga Nasional, Malaysia*

^{a)} Corresponding author: irsyad.a.aa@gmail.com

Abstract. A solar thermochemical reactor is a device utilizing concentrated solar energy to conduct hydrogen gas production by two-step water-splitting by dissociation of a reactive material, such as zinc oxide (ZnO). Reactor design, heat transfer, and reaction kinetics contribute a significant portion to the achievement of high solar-to-fuel conversion efficiency. In this work, an investigation of an indirect-cavity type reactor design performance has been conducted by numerical simulation method by coupling the computational model of fluid flow, energy equation, discrete ordinate radiation, and species transport. The reactor consisted of a windowed cavity reactor with an array of five tubes containing the flow of the reactive material. Dissociation of ZnO in a steady state condition of the reactor has been assessed under 1,500 sun heat flux from quartz window. A parametric study has been performed for a variation of the particle's mass flow rate, solar flux peak in, and reactor configuration. The cavity of the reactor was insulated by a ceramic and reflective material to reduce the conduction and radiation losses. Inert gas of Ar was injected into the tube as product carrier. Energy balance analysis and reactor efficiency calculation have been performed to analyze the reactor performance. The results showed that the thermal re-radiation through the window and thermal conduction through the cavity wall dominated the heat losses around 84 % in total. The best operating condition in this study was at a mass flow rate 0.05 g/s, peak-heat-in 2,000 kW/m², and tubes configuration of the staggered-front dominant. Some recommendations to improve the research include changing the chemical reactant with other metal-oxide which has a lower reactivity, increasing the tubes number to absorb the solar irradiation, combining the metal-oxide decomposition with other processes which require less heat, and applying the special material in window side which can filter the high wavelength from going outside the reactor to decrease the re-radiation losses.

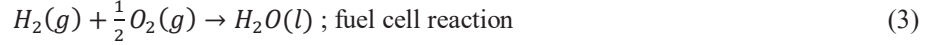
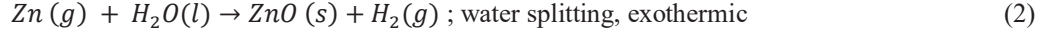
INTRODUCTION

Energy demand has been increased each year, and fossil fuel has become the main energy source around the world to fulfill the energy demand [1]. Fossil fuel has two big demerits, which is its limited availability and the carbon dioxide emission from the fossil fuel combustion. Global carbon dioxide concentration has been increased from 330 ppm in 1970 to 390 ppm in 2017 which leads to increasing global temperature at 1 °C [1]. Some of the solutions pushed for decreasing the carbon production are: using a better technology for combustion to reduce greenhouse gas emission, limit the usage of fossil fuel, increase the efficiency of combustion, and increase the usage of renewable energy.

Hydrogen can be utilized as clean energy carrier due to high energy density, generate electricity when powering a fuel cell, and the reaction product is water which environment-friendly. However, hydrogen gas production is still dominated from fossil fuel as the origin of hydrogen, and the extraction of the hydrogen gas requires a high amount of energy which also comes from fossil fuel [2].

Concentrated solar energy could achieve high temperature needed for two-step water splitting by reduction-oxidation by metal-oxide. There are already many metal oxide considered for two-step water splitting for producing hydrogen gas such as ZnO/Zn, SnO₂/Sn, CeO₂/Ce₂O₃, and M_xFe_{1+x}O₄. Zinc oxide, among them, has been gaining

the highest attention in previous works due to high H₂ production and its reaction kinetics has been studied extensively which provide the reliable data [3-10]. The cyclic process of reaction for two-step water splitting using zinc oxide decomposition and utilization of hydrogen gas for a fuel cell is described in (1)-(3).



From many research mentioned above, there is still few investigation of the indirect-type receiver which can solve the problem chemical deposition in the cavity wall that can reduce the performance of the reactor.

In this study, a computational model of fluid flow, heat transfer, radiation, and chemical kinetics is developed to investigate the performance of an indirect-type receiver using finite volume analysis of computational fluid dynamics (CFD). Parametric study of the varying operating condition and tubes configuration also investigated to find the best performance of the reactor.

MODELLING OF INDIRECT-TYPE RECEIVER

Governing Equations

The related equation used in the CFD describe by the set of continuity, momentum, and energy equations. The continuity equation is given by [11].

$$\frac{\partial \rho}{\partial t} + \frac{\partial}{\partial x_i}(\rho v_i) = S_m \quad (4)$$

Conservation of momentum in *i* direction is given by [11].

$$\frac{\partial}{\partial t}(\rho \cdot v_i) + \frac{\partial}{\partial x_i}(\rho \cdot v_i \cdot v_i) = \frac{\partial p}{\partial x_i} + \frac{\partial \bar{\tau}}{\partial x_i} + \rho g_i + F_i \quad (5)$$

$\bar{\tau}$ define as a tensor of shear stress which can be calculated by the equation [11].

$$\bar{\tau} = \mu \left[\left(\frac{\partial v_i}{\partial x_j} + \frac{\partial v_j}{\partial x_i} \right) - \frac{2}{3} \cdot \frac{\partial v_k}{\partial x_k} I \right] \quad (6)$$

The energy equation in the simulation which involves the heat transfer is given by [11].

$$\frac{\partial}{\partial t}(\rho E) + \frac{\partial}{\partial x_i}(v_i(\rho E + p)) = \frac{\partial p}{\partial x_i} \left(k_{eff} \frac{\partial T}{\partial x_i} - \sum_j h_j \cdot j_j + \left(\bar{\tau}_{eff} \cdot v_j \right) \right) + S_h \quad (7)$$

With k_{eff} is effective conductivity, $k_{eff} = k + k_t$.

Radiative transfer equation can be solved by a finite number of discrete solid angles in Discrete Ordinate (DO) model. The solution method is the same as the fluid flow and energy equation. The DO model for gray model radiation is

$$\nabla \cdot (I_{rad}(\bar{r}, \bar{s})\bar{s}) + (a + \sigma_s)I_{rad}(\bar{r}, \bar{s}') = an^2 \frac{\sigma T^4}{\pi} + \frac{\sigma_s}{4\pi} \int_0^{4\pi} I_{rad}(\bar{r}, \bar{s}')\Phi(\bar{s}, \bar{s}')d\Omega' \quad (8)$$

Each octant of angular space 4π at any spatial location is discretized into $N_\theta \times N_\phi$ solid angles with extent ω_p as control angles. θ and ϕ are polar and azimuthal angles. In three-dimensional calculation, a total of $8 N_\theta \times N_\phi$ the direction is solved.

The discrete ordinate criteria for the Fluent setting referred to Moghimi et al. which comparing the discrete ordinate method for solving radiative transfer properties and compare it to Monte Carlo Ray Tracing method [12]. The shortcoming of the discrete ordinate method which involving the ray effect and false scattering has been eliminated by putting the radiation setting by increasing the control angle count, spatial mesh count, and using higher order spatial discretization scheme for the DO direction equations. The DO discretization of 3×50 pixel solved in $8 N_\theta \times N_\phi$ considered as enough to get the valid result [12].

Arrhenius law is used for the reaction kinetics with the kinetic rate of species reaction, r_{kin} , per unit area is

$$r_{kin} = A_r \exp\left(\frac{-E_a}{RT}\right) \quad (9)$$

Receiver Model

The reactor is indirectly irradiated tubular reactor with window. The advantage of indirect reactor type is to minimize the depleted chemical in the cavity wall or reactor window which may affect to decrease the reactor performance and higher cost for reactor maintenance. With clean cavity wall, some modification of reactor wall can be done such as making the cavity wall as a reflective or an absorbing wall. In this research, the cavity wall determined as absorbing wall.

A preliminary study was indirect-reactor with one tube as shown in Figure 1 to simplified the setting and reduced the computational cost. The diameter of the reactor was 150 mm, and the height is 240 mm. The opening window as the way of entering solar irradiation was 51.3 mm x 80 mm. Tube diameter is 25.4 mm. The setting of mesh, material definition, boundary condition, and solution method has been done to meet the proper calculation result.

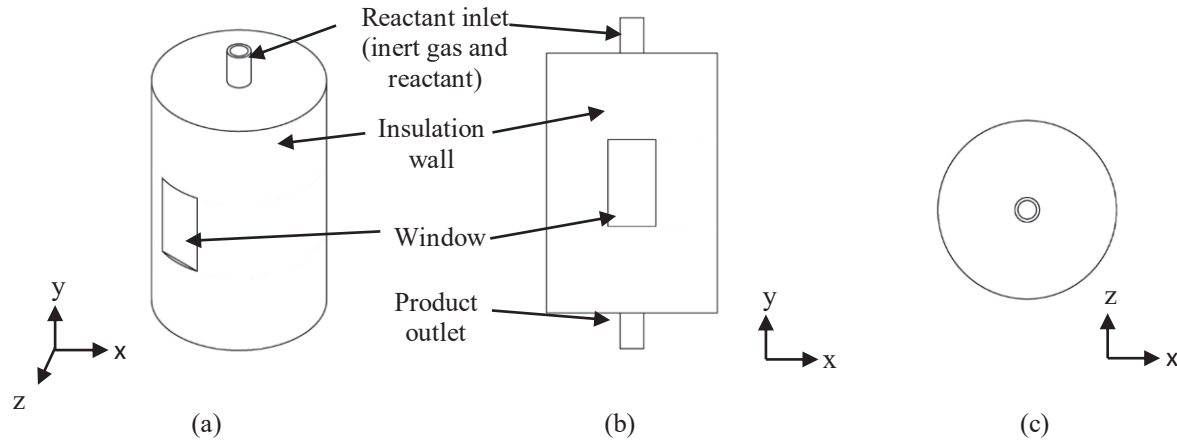


FIGURE 1. Sketch drawing on reactor design for preliminary study (a) isometric view, (b) x-y axis, and (d) x-z axis

TABLE 1. Thermophysical properties of materials

Properties	Air	Ceramic	Zinc-oxide	SiC	Quartz glass
Density [kg.m ³]	Ideal gas	3900	5600	3091	2725
Heat capacity [J.kg ⁻¹ .K ⁻¹]	1206.78	1274.5	$300.5 + 0.4T - 4.9e^{-4}T^2 + 2.5e^{-7}T^3 - 4.7e^{-11}T^4$	$715.34 + 0.826T - 4.399e^{-4}T^2 + 1.164e^{-7}T^3 - 1.184e^{-11}T^4$	$980.886 + 0.167T$
Thermal conductivity [W/m.K]	0.0242	$35.245 - 0.0353T - 1.31e^{-5}T^2 - 1.73e^{-9}T^3$	0.2	60	3.4

Material included in the computational model consisted of solid, liquid, and mixture phase. The solid phase consisted of alumina Al_2O_3 as an insulator of the cavity wall, silicon carbide SiC which have excellent durability in the high-temperature heat transfer operation as tube material, and quartz glass as a window of the reactor. Fluid phases inside the cavity were air. Argon gas used in the preliminary study and parametric study as inert gas carrying reactant. Zinc oxide assumed as gas phase, and gas product consisted of zinc and oxygen. The temperature dependence of some properties was considered in calculations and shown in Table 1. The mixture of gas was considered as an ideal mixture.

Boundary Condition

Equation (4)-(8) was solved in a steady state condition in a commercial CFD software, ANSYS Fluent 15. The appropriate boundary condition was set to do the accurate numerical calculation of the finite volume analysis of the reactor. Cavity wall modeled as absorbing wall with temperature boundary condition at 300 K. In the real reactor, it means that the reactor wall was receiving active cooling in the wall to prevent excess heat losses into the surrounding atmosphere. Low temperature lowered the re-radiation losses.

The reactor's window was set as semi-transparent media and gave the direct solar irradiation with peak 2,000 kW/m^2 . It was assumed there is no diffusion in the radiation. The interface between fluid cavity and tube wall was set as coupled. Inlet of the tube defined as mass flow inlet with mass flow rate at 0.5 g/s. The outlet of the tube defined as pressure outlet with atmospheric pressure. In the case of zinc oxide, the study of the reaction kinetics has been done by Palumbo which result to $E_a = 356$ kJ/mol and $A_r = 4 \times 10^9$ s^{-1} [10].

Irradiation boundary condition considered from a solar concentrating plant of High Flux Solar Furnace (HFSF) by National Renewable Energy Laboratory (NREL) was considered in this research as the concentrated solar source. HFSF was modeled in a Monte Carlo Ray Tracing (MCRT) freeware developed and coded by NREL. Calculation of ray tracing for 1,000,000 rays gave the solar flux contour of Gaussian distribution with the peak of solar flux at 2,000 kW/m^2 . The result was in agreement with the experimental result from NREL [13]. The method used for exporting the solar irradiation flux was based on Craig et al. which discretized the surface of the window into several faces split and input each face with the irradiation condition [14-15]. This method has been validated by the MCRT method.

A parametrical study has been performed to see the effect of some parameters on the reactor performance. The mass flow rate is varying at 0.5 g/s, 0.1 g/s, and 0.05 g/s. The solar irradiation is assumed at 2,000 and 6,000 kW/m^2 .

Tubes Configuration

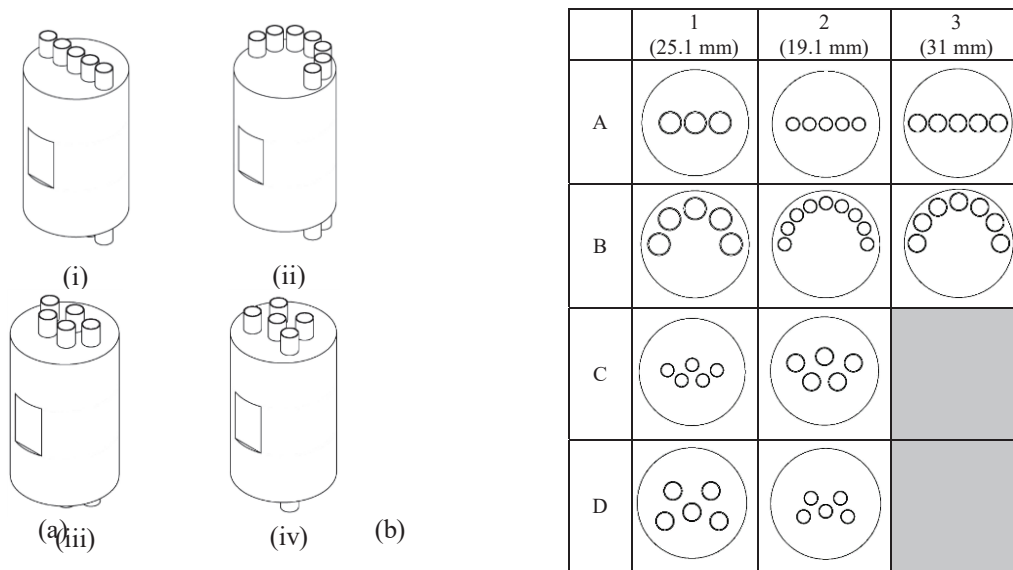


FIGURE 2. (a) Variation of tubes configuration inside reactor for parametric study, (i) configuration A, (ii) configuration B, (iii) configuration C, and (iv) configuration D and (b) variation of diameter for each configuration in x-z plane

A parametrical study by varying the tube configuration has been performed to see the different performance in a different configuration. Tube configuration was determined respectively for Figure 2 (a) from (i) to (iv) which were as straight configuration perpendicular to the window, half-circumference, staggered back-dominant, and staggered front-dominant. The tube diameter of each tube also varied at 25.4 mm, 19.1 mm, and 31 mm to know the effect on heat transfer. It can be seen in Figure 2 (b) which the code for future discussion was based on the intersection of row and column, which is A1, A2, A3, B1, B2, B3, C1, C2, D1, and D2.

Grid Convergence Study

The grid convergence has been studied to see the calculation result difference between coarser with finer mesh. The total number of the element for coarse and fine mesh respectively were 70,294 and 140,503. The calculation performed in ANSYS Fluent. The difference between two cases was less than 10 K. From this result, we can set all the mesh portrayed in the research in coarse level to make the calculation faster and lower the computational cost.

RESULT AND DISCUSSION

Preliminary Result

From Figure 3 (a), the concentrated solar radiation hit three tubes, and the heat flux became higher in those tubes. It affected the temperature of the fluid which can be seen in Figure 3 (b). The fluid was receiving heat from the cavity reactor by conduction, convection, and radiation heat transfer modes. The temperature was developed from 300 K in the inlet side into 2000 K on the outlet side. The temperature of the fluid reached 2,000 K which was the required temperature to perform thermal decomposition reaction of ZnO. Each tube has maximum difference temperature shown in Figure 3 (c). The temperature difference was around 400 K for tube 2 and tube 1-4. The temperature of tube 3 reached 1,000 K and tube reach 1,400 K. The tube which intercepts solar irradiation directly obtained the higher temperature than the others.

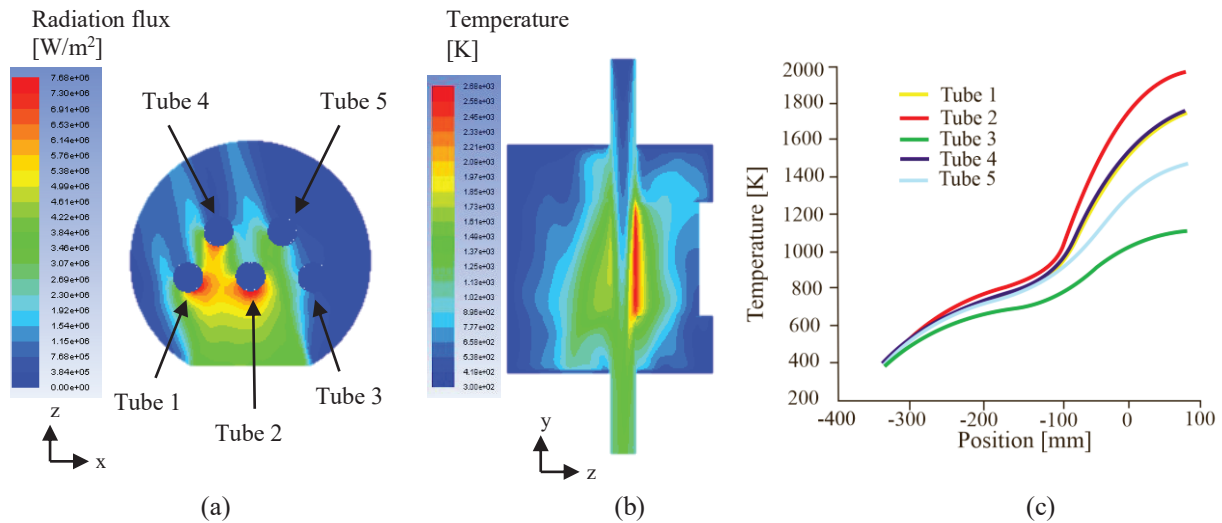


FIGURE 3. (a) Contour of incident radiation flux in W/m^2 , (b) contour of temperature in K, and (c) chart of temperature vs. tube distance along y-axis of the reactor

The next step was to analyze the mass and energy balance inside the reactor. It has been confirmed that the mass balance net was zero by calculating the net of mass flow rate between the outlet and inlet of tubes. The energy inside the reactor was transferred to the tubes containing the reacting flow, and the excess heat will be transferred to the reactor wall by conduction and reradiated to the outside reactor through the window.

The heat losses inside the reactor were relatively large, with conduction losses to cavity wall at 3300 W (43 %) and re-radiation through quartz window at 3214 W (41.9 %). The efficiency of heat transfer inside the reactor was defined as total heat transferred into tube divided by total heat entering the reactor. From this preliminary study, the efficiency of the staggered tube was 15.2 %. This number agrees with some of another researchers' results [3-4, 6] with the different configuration. The heat loss was very high because the majority of energy was brought by the electromagnetic waves in high temperature. The summary of energy balance shown in Table 2.

TABLE 2. Energy Balance Inside Reactor and The Heat Used for Thermal Decomposition of ZnO

Geometry	Heat transfer rate [W]	Percentage heat Transferred [%]	Chemical conversion [W]
Cavity wall	3300	43	-
Quartz window	3214	41.9	-
Tube 1	218	2.8	33
Tube 2	361	4.7	251
Tube 3	178	2.3	5
Tube 4	210	2.7	32
Tube 5	193	2.5	9
TOTAL	7676	100	-

The chemical conversion from ZnO to Zn and O₂ also performed in this preliminary study. The efficiency of chemical conversion in each tube was around 28.4 % from the heat transferred into the tube, and around 4.3 % of the heat entered the reactor. This value was shallow because the high-temperature condition should be achieved to perform the thermal decomposition of ZnO. Based on this result, it is recommended to change the fluid into another metal oxide which has a lower enthalpy of reaction to performing two-step water splitting. This amount of heat can also be used for steam reforming from methane to syngas which only requires fluid temperature around 1200 K. It also recommends the other tubes operate another process which requires less heat such as heating water, conversion of water-to-steam, heating phase change material (PCM), and thermal storage purpose.

The challenge of high heat losses can be solved by changing the window material in the future. The desired window material should have the ability to filter the radiation which goes out from the reactor. Within the high-temperature range, the longer wavelength will remain inside the reactor. This method can be combined by applying the cavity wall insulation which has an appropriate value of reflectivity in high-temperature wavelength. The one component which should receive more energy is the tube. To obtain this, the more installed tube inside the cavity may reduce the unused heat losses because it increases the surface of heat transfer area. Even if the temperature increment is not as high as the tube which directly intercepts the solar irradiation, it can be useful for another purpose as described in below paragraph.

Parametric Studies

Operating Condition

Some of the operating conditions were modified into designated value to understand the effect of mass flow rate and the heat entered the reactor. It was predicted with lower velocity lead to higher efficiency of heat transfer and chemical conversion because the fluid has a longer time to receive the heat. It was also expected with higher energy enter the reactor led to higher efficiency due to more energy was transferred into the tube. The calculation was shown in Table 3.

TABLE 3 Parametric Study Result for Varying Mass Flow Rate at Inlet and Peak Solar Flux Entering the Reactor

PARAMETER	2,000 kW/m ²			6,000 kW/m ²		
	0.5 g/s	0.1 g/s	0.05 g/s	0.5 g/s	0.1 g/s	0.05 g/s
Heat transfer efficiency (%)	15.2	17.3	17.6	7.2	8.4	8.9
Tube-to-chemical efficiency (%)	28.4	32.3	33.8	29.7	31.2	32.4
Total efficiency (reactor-to-chemical) (%)	4.3	5.6	6.0	0.2	0.3	0.5

The variation of mass flow rate met the expectation. With lowest flow rate at 0.05 g/s increased the heat transfer efficiency around 2 % and lower flow rate at 0.1 g/s increase the heat transfer efficiency around 1 %. The difference was not significant in each value because the flow was laminar with low thermal conductivity.

The result of variation of energy-in did not meet the expectation. The heat transfer efficiency decreased around 9 %. The higher energy-in to the reactor makes higher energy transferred into the tube, but it was also affected by increasing of heat losses. It can be concluded that specific reactor geometry, tube configuration, and size had each optimum operating condition. Based on the literature [3-4, 6], the conclusion was confirmed. Based on the parametric study above, the operating condition which brings the best result were the mass flow-rate-in at 0.05 g/s and radiation peak-flux-in at 2,000 kW/m².

Tubes Configuration

The second parametric study to know the heat transfer performance was performed by comparing the tubes configuration inside the reactor. The desired geometry has been shown in subsection 3.3. There were four configurations, and each configuration has their diameter variation as explained in subsection 3.3. We compared each configuration with the solar irradiation is at the peak of a sunny day with concentrated solar flux peak is 2,000 kW/m². The direction was perpendicular to the reactor window and magnitude of concentrated solar irradiation shown in Figure 4.

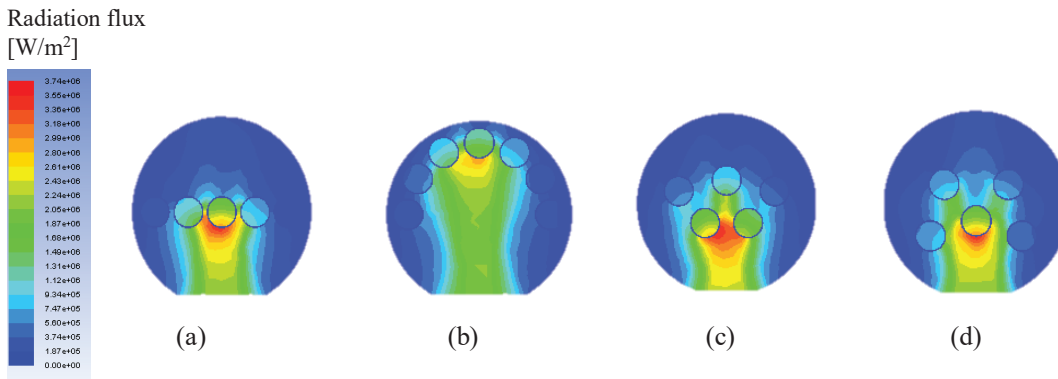


FIGURE 4. Configuration (a) A, (b) B, (c) C, and (d) D which receive direct irradiation magnitude in sunny peak day in W/m²

After the calculation finished and the result is processed, the summary of calculation of heat transfer balance was described in Table 4.

TABLE 4. Summary of Configuration Performance Comparison Between A, B, C, and D Type in a Sunny Peak Day

Confi- guration	Total tube heat transfer rate	Heat transfer efficiency	Heat losses to a cavity	Heat losses by re-radiation
	[W]	[%]	[%]	[%]
A1	630	7.9	45.6	46.5
A2	1,504	16.7	41.3	42.0
A3	888	10.7	43.9	45.4
B1	953	10.9	44.1	45.0
B2	953	10.8	44.1	45.1
B3	1,423	15.4	41.4	43.2
C1	1,252	14.6	41.6	43.7
C2	1,312	15.1	41.4	43.5
D1	1,873	20.4	39.3	40.3
D2	1,933	20.7	39.2	40.2

From this result, the highest efficiency of heat transfer for the same diameter at 25.4 mm (code 1) was obtained, from the highest to the lowest were D, C, B, and A. It was happened due to there were many areas of tube surfaces intercepted the solar irradiation directly in staggered-front dominant (D) configuration. The shading case also considered as good case which made the back tube could increase the fluid temperature; it made the total heat absorbed was higher. In the perpendicular of radiation-in, the straight configuration (A) will have fewer surface area intercepted by the radiation-in.

In the case of the effect of tubes diameter, each configuration has their preference. The straight (A) configuration have the more efficient in the smaller tube due to larger surface tubes intercept the direct solar irradiation. In the bigger tube diameter at 31 mm, the surface area intercepted by the tube was fewer than on 25.4 mm and 19.1mm. With the bigger diameter, the tube fitted in the reactor was limited to three which can be considered as the cause of less heat transferred.

In the half-circumference (B) tube, the larger the tube size made the higher efficiency. The efficiency of heat transfer respectively for 19.1 mm, 25.4 mm, and 31 mm were 10.8 %, 19.9 %, and 15.4 %. The surface area of tube intercepted the direct irradiation from the window was a little bit higher than the A configuration. It was expected due to its position near the reactor wall which received the solar reflection from the cavity wall. With the bigger tube, the surface area for receiving heat transfer from direct irradiation and reflection from cavity wall surface was increased.

In the case of a staggered tube (C and D), the difference was not as significant as straight and half-circumference configuration. It was due to similar surface area intercepted the direct and reflected solar radiation from all direction. The front-dominant tube has the higher efficiency due the tubes intercept the first solar irradiation far greater than the back-dominant. The bar-chart version of Table 3 can be seen in Figure 5.

From a parametric study of tubes configuration, the best performance of the receiver achieved by the staggered-front dominant (D) configuration at tubes diameter 25.1 mm. The better result of efficiency should be attained by applying the special window glass material for filtering radiation out from the reactor to reduced the reradiation heat loss, suitable reflective material for cavity wall to reduced the thermal conduction loss, installed as many tubes to absorb heat transferred into the reactor, utilize the less heat transferred tube with other application, and operated the reactor in the best optimum condition.

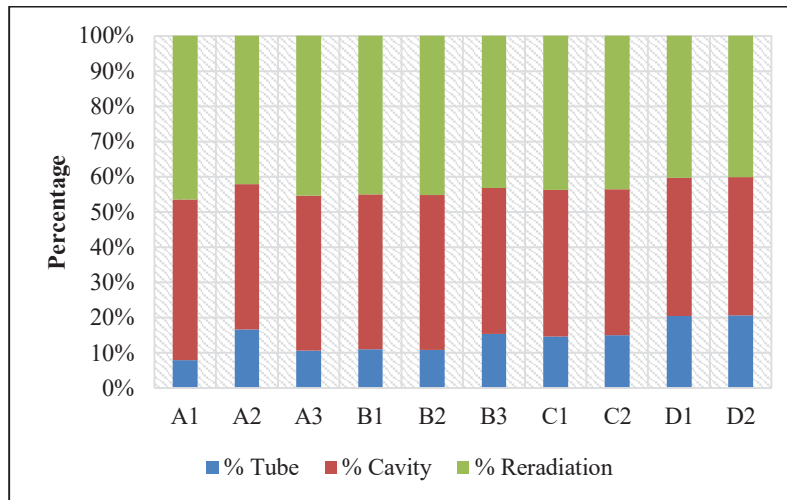


FIGURE 5. Chart of heat balance for configuration A1-D2

CONCLUSION

The coupled numerical model in ANSYS Fluent 15 for the solar thermochemical reactor to evaluate thermal decomposition of ZnO has been performed. The simulation was in steady state condition which involving the continuity equation, energy equation, momentum equation, species transport, Arrhenius law, and radiation discrete ordinate method.

A preliminary study was done by a five-staggered tube with mass flow rate at 0.5 g/s and irradiation flux peak at 2000 kW/m². The heat transfer efficiency from the reactor into the tube is 15.2 %, and overall chemical conversion efficiency was 4.3 %. The heat losses were dominated by thermal conduction through the reactor wall and re-radiation through the reactor's window.

The parametrical study on operating condition has been done. The lower mass-flow-in increased the efficiency in maximum 2.4 % due to extending the time for the fluid receiving heat, and the laminar condition of the fluid made no different by increasing the mass-flow-in. The higher solar irradiation peak flux at 6000 kW/m² decreased the efficiency up to 9 % due to more heat losses into the cavity wall and re-radiation through the window. The best operating condition from this study was at mass-flow-in 0.05 g/s and solar-flux-in at 2,000 kW/m².

The parametrical study on reactor configuration and geometry has been done. The staggered configuration with front-dominant (D) tube has the highest efficiency in both peak condition and average day condition. It was followed by staggered-back-dominant. The straight (A) configuration reached the higher efficiency in the smaller tube, and the half-circumference (B) configuration reached the higher efficiency in the larger tube. It can be said that this two configuration has their preference for the optimum tube size.

The future works which can be expanded from this research are:

- Modifying the reactive chemical. It can be said that this research cannot reach the expected result of thermal decomposition of ZnO due to its high energy required.
- Combining the metal-oxide decomposition process with another process which requires lower energy and temperature such as heating phase change material (PCM), steam reforming, air heating for a gas turbine, and thermal storage purpose.
- Focusing on the development of window material to reduce the re-radiation losses from the reactor. Such solution may consider the wavelength properties of radiation. The cavity wall should be modified as a reflective window to reduce the radiation absorbed into the cavity wall.

ACKNOWLEDGMENTS

The first author acknowledges the support from Indonesia Endowment Fund for Education (LPDP RI).

NOMENCLATURE

ρ	density (kg m ⁻³)	C	concentration ratio at receiver aperture
p	pressure (atm)	σ	Stefan-Boltzmann constant (5.672 * 10 ⁻⁸ W m ⁻² K ⁻⁴)
T	temperature (K)	N_θ	pixelation in θ direction
t	time (s)	N_φ	pixelation in φ direction
v	fluid velocity (m s ⁻¹)	\vec{r}	position vector (m)
x	position (m)	\vec{s}	direction vector (m)
S_m	mass source term (kg m ⁻³ s ⁻¹)	Ω'	solid angle (rad)
g	gravity acceleration (m s ⁻²)	A_r	pre-exponential factor (kg m ⁻² s ⁻²)
$\bar{\tau}$	tensor of shear stress	E_a	activation energy (J mol ⁻¹)
k_{eff}	effective conductivity (W m ⁻¹ K ⁻¹)	\tilde{R}	universal gas constant (8.314 J K ⁻¹ mol ⁻¹)
k	thermal conductivity (W m ⁻¹ K ⁻¹)	μ	molecular viscosity (kg m ⁻¹ s ⁻¹)
k_t	thermal conductivity in turbulent (W m ⁻¹ K ⁻¹)	I	tensor unit
E	energy (internal, potential, kinetic) (W)	Φ	scattering phase function
S_h	volumetric heat source term (W m ⁻³)	a	absorption coefficient (m ⁻¹)
n	real part of refractive index	\vec{s}'	scattering direction vector (m)
σ_s	scattering coefficient (m ⁻¹)	λ	wavelength (m)
I_{rad}	radiation intensity, depends on \vec{r} and \vec{s}		

REFERENCES

1. <https://www.bp.com/content/dam/bp/pdf/energy-economics/energy-outlook-2017/bp-energy-outlook-2017.pdf>
2. A. Zuttel, A. Remhof, A. Borgschulte, & O. Friedrichs. "Hydrogen: the future energy carrier," in *Philosophical Transactions of the royal society*, 368, 3329-3342 (2010).
3. S. Abanades, P. Charvin, & G. Flamant, "Design and simulation of a solar chemical reactor for the thermal reduction of metal oxides: a Case study of zinc oxide dissociation," in *Chemical Engineering Science*, 62, 6323-6333 (2007).
4. J. P. Muthusamy, S. Abanades, T. Shamim, & N. Calvet, "Numerical modeling and optimization of an entrained particle-flow thermochemical solar reactor for metal oxide reduction," in *Energy Procedia*, 69, 947-956 (2015).
5. J. F. Klausner, L. Li, A. Singh, N. Yeung, R. Mei., D. Hahn, & J. Petrasch, "The role of heat transfer in sunlight to fuel conversion using high temperature solar thermochemical reactors," in International Heat Transfer Conference, IHTC 15. Kyoto (2014).
6. K. S. Reddy, D. Premkumar, & T. Vikram, "Heat transfer modeling and analysis of solar thermochemical reactor for hydrogen production from water," in *Energy Procedia*, 57, 570-579 (2014).
7. H. Kaneko, Y. Ishikawa, C. Lee, G. Hart, W. Stein, & Y. Tamaura, "Simulation study of Tokyo-tech rotary type solar reactor on solar field test at CSIRO in Australia," in ASME 5th International Conference on Energy Sustainability. Washington (2011).
8. S. Rodat, S. Abanades, J. Sans, & G. Flamant, "Hydrogen production from solar thermal dissociation of natural gas: development of a 10 kW solar chemical prototype," in *Solar Energy*, 83, 1599-1610 (2009).
9. L. O. Schunk, & A. Steinfeld. "Kinetics of the thermal dissociation of ZnO exposed to concentrated solar irradiation using a solar-driven thermogravimetric in the 1800-2100 K range," in *American Institute of Chemical Engineers*, 55 (2009).
10. S. Moller & R. Palumbo, "Solar thermal decomposition kinetics of ZnO in the temperature range 1950-2400 K," in *Chemical Engineering Science*, 56, 4505-4515 (2001).
11. ANSYS Fluent Theory Guide. (2013).
12. M. A. Moghimi, K. Craig, & J. Meyer, "A novel computational approach to combine the optical and thermal modeling of Linear Fresnel Collectors using the finite volume method," in *Solar Energy*, 116, 407-427 (2015).
13. A. Lewandoski, C. Bingham, J. O'Gallagher, R. Winston, D. Sagie, "Performance characterization of the SERI High-Flux Solar Furnace," in *Solar Energy Materials*, 24, 550563 (1991).
14. K. J. Craig, P. Gauche, & H. Kretschmar, "CFD analysis of solar tower Hybrid Pressurized Air Receiver (HPAR) with a dual-banded radiation model," in *Solar Energy*, 110, 338-355 (2014).
15. S. S. Khalsa, & C. Ho, "Development of a "solar patch" calculator to evaluate heliostat-field irradiance as a boundary condition in CFD models," in ASME 2010 4th International Conference on Energy Sustainability. Phoenix, Arizona: ASME (2010).